



Electrogenic steps of light-driven proton transport in ESR, a retinal protein from *Exiguobacterium sibiricum*

Sergey A. Siletsky^{a,*}, Mahir D. Mamedov^a, Evgeniy P. Lukashev^b, Sergei P. Balashov^{c,**}, Dmitriy A. Dolgikh^{b,d}, Andrei B. Rubin^b, Mikhail P. Kirpichnikov^{b,d}, Lada E. Petrovskaya^{d,***}

^a Belozersky Institute of Physical-Chemical Biology, Lomonosov Moscow State University, 119991 Moscow, Russian Federation

^b Department of Biology, Lomonosov Moscow State University, 119234 Moscow, Leninskie gory, 1, Russian Federation

^c Department of Physiology and Biophysics, University of California, Irvine 92697, USA

^d Shemyakin & Ovchinnikov Institute of Bioorganic Chemistry, Russian Academy of Sciences, 117997, Moscow, Ul. Miklukho-Maklaya, 16/10, Russian Federation

ARTICLE INFO

Article history:

Received 27 May 2016

Received in revised form 6 August 2016

Accepted 11 August 2016

Available online 12 August 2016

Keywords:

Retinal protein

Light energy transduction

Proton pump

Photocycle

Photoelectric potential generation

Charge transfer steps

ABSTRACT

A retinal protein from *Exiguobacterium sibiricum* (ESR) functions as a light-driven proton pump. Unlike other proton pumps, it contains Lys96 instead of a usual carboxylic residue in the internal proton donor site. Nevertheless, the reprotonation of the Schiff base occurs fast, indicating that Lys96 facilitates proton transfer from the bulk. In this study we examined kinetics of light-induced transmembrane electrical potential difference, $\Delta\Psi$, generated in proteoliposomes reconstituted with ESR. We show that total magnitude of $\Delta\Psi$ is comparable to that produced by bacteriorhodopsin but its kinetic components and their pH dependence are substantially different. The results are in agreement with the earlier finding that proton uptake precedes reprotonation of the Schiff base in ESR, suggesting that Lys96 is unprotonated in the initial state and gains a proton transiently in the photocycle. The electrogenic phases and the photocycle transitions related to proton transfer from the bulk to the Schiff base are pH dependent. At neutral pH, they occur with τ 0.5 ms and 4.5 ms. At alkaline pH, the fast component ceases and Schiff base reprotonation slows. At pH 8.4, a spectrally silent electrogenic component with τ 0.25 ms is detected, which can be attributed to proton transfer from the bulk to Lys96. At pH 5.1, the amplitude of $\Delta\Psi$ decreases 10 fold, reflecting a decreased yield and rate of proton transfer, apparently from protonation of the acceptor (Asp85–His57 pair) in the initial state. The features of the photoelectric potential generation correlate with the ESR structure and proposed mechanism of proton transfer.

© 2016 Elsevier B.V. All rights reserved.

1. Introduction

Microbial retinal protein family includes numerous light-activated pumps, channels and sensors, which share a similar topology of seven transmembrane alpha-helical segments and an all-*trans* retinal chromophore connected through the Schiff base linkage to a conserved lysine residue [1–3] but differ in the set of residues specific for their function. Upon photon absorption, the retinal undergoes isomerization

from all-*trans* to a twisted 13-*cis* configuration. It induces a series of conformational relaxations of a protein, which returns to the initial state after reisomerization of the chromophore back to all-*trans* [4]. Light energy accumulated in the primary light reaction is utilized for translocation of protons or other ions by pumps [3,5], gating of ion conductance by channelrhodopsins [6,7] or signaling event by sensory rhodopsins [1–3,8].

In bacteriorhodopsin from *Halobacterium salinarum* (BR), the most studied bacterial retinal protein, few key carboxylic amino acid residues are directly involved in proton pumping, acting as a proton acceptor from the Schiff base (Asp85), a proton donor to the Schiff base (Asp96) and a proton releasing complex comprised of Glu194, Glu204 and bound waters, interacting with Arg82, and through the latter, with Asp85 [5,9–11]. The counterion to the Schiff base and proton acceptor Asp85 is indispensable for proton pumping. Mutation of this residue eliminates transport of protons [12]; mutations of others affect mainly the rates of proton transport [9,13,14] or the pK_a of Asp85, as it does the mutations of Arg82 [12]. During the photocycle, the characteristic pK_a s of these residues as well as that of the Schiff base undergo

Abbreviations: BR, bacteriorhodopsin; ESR, retinal protein from *Exiguobacterium sibiricum*; PR, proteorhodopsin; XR, xanthorhodopsin; DDM, n-dodecyl- β -D-maltopyranoside; HEPES, 4-(2-Hydroxyethyl)piperazine-1-ethanesulfonic acid; OG, octyl- β -D-glucopyranoside; PRG, proton releasing group.

* Corresponding author.

** Correspondence to: S.P. Balashov, Dept. of Physiology and Biophysics, C-335 Medical Sciences I, University of California, Irvine, CA 92697-4560, USA.

*** Correspondence to: L.E. Petrovskaya, Shemyakin and Ovchinnikov Institute of Bioorganic Chemistry, ul. Miklukho-Maklaya, 16/10, 117997 Moscow, GSP-7, Russian Federation.

E-mail addresses: siletsky@genebee.msu.su (S.A. Siletsky), balashov@uci.edu (S.P. Balashov), lpetr65@yahoo.com (L.E. Petrovskaya).

changes leading to proton transport from the cytoplasmic surface of the protein to its extracellular side, which occurs in several distinctive steps [9,15].

Eubacterial proton pumps (variants of proteorhodopsin and xanthorhodopsin) exhibit several differences from bacteriorhodopsin in the architecture of proton conducting pathways [16,17]. They contain a conserved histidine residue participating in strong hydrogen bonding with the proton acceptor [18,19] thus affecting its pK_a , taking over the function of Arg82 in this regard. At the internal proton donor site, the aspartic acid residue is replaced with a glutamic [2,16]. At the extracellular side the key components of proton release complex, the Glu194-Glu204 pair of residues, are not strictly conserved in PRs and XR, which results in elimination of early proton release following protonation of the counterion as it is observed in BR. Release of a proton occurs at the last step of the photocycle upon deprotonation of the counterion [2,3,20,21].

The presence of a carboxylic residue at the donor site (Asp96 in BR) was considered as a hallmark of proton pumps [22]. Its function is facilitation of proton conductance from the cytoplasmic surface to the Schiff base [23]. Surprisingly, in the retinal protein from *Exiguobacterium sibiricum* (ESR), which showed substantial homology to BR, PR and XR (30%, 34% and 33%, respectively), a lysine residue (Lys96) was found in the position corresponding to the proton donor to the Schiff base [24,25]. This raised the question on whether ESR is a pump or a sensor and what is the function of Lys96. Later more variants of ESR with Lys in the donor site were found in various environments [26,27] different from permafrost soil where *E. sibiricum* was discovered [28].

We have expressed ESR in *Escherichia coli* cells and showed that the protein functions as a proton pump [24]. It undergoes a photocycle similar to that of BR [29] and PR [21], which includes several spectrally identified photointermediates: ESR \rightarrow K \rightarrow L \rightarrow M1 \leftrightarrow M2 \leftrightarrow N1 \leftrightarrow N2/O \rightarrow ESR [24,30,31], where K and L are early intermediates with 13-*cis* chromophore; the M intermediate is a state with deprotonated Schiff base and protonated counterion; the N1 and N2 states are formed after reprotonation of the Schiff base; and O is a state after reisomerization of the chromophore, which is present in a mixture with the N states; ESR stands for the initial unphotolysed state.

It was shown that Lys96 facilitates reprotonation of the Schiff base, acting as a proton donor [32]. The proposed sequence of the proton transfer events following retinal isomerization in ESR includes deprotonation of the Schiff base (formation of the M intermediate) and protonation of Asp85, proton uptake from the bulk by the donor site including Lys96 and subsequent reprotonation of the Schiff base (during the decay of the M intermediate). The unusual sequence when proton uptake from the bulk precedes Schiff base reprotonation [32] indicates that in contrast to Asp96 of BR, and Glu107 in PR, Lys96 in ESR is unprotonated in the initial state at neutral pH, consistent with its mostly hydrophobic environment revealed by crystal structure of ESR [33], and gains a proton transiently during the photocycle. Large solvation energy of ionizable residues such as Lys and Asp buried in proteins results in large pK_a shifts of ca. 4–5 (increase for negatively charged Asp and decrease for Lys), so that at neutral pH both acid and alkaline residues are uncharged in hydrophobic environment [32,34]. The pK_a of these residues and their protonation state but might be strongly influenced by interaction with water molecules during the photocycle. Proton release at the extracellular side of ESR takes place at the last step of the photocycle [30], similar to PR [35] and BR mutants in which the proton release complex is absent [36] and indicating that ESR, as PR and XR, lacks specialized proton release complex found in BR [2,9,14,20,30].

Further insight into the mechanism of intramembrane proton transfer in ESR and especially the steps associated with the function of unusual donor, Lys96, can be gained by time-resolved potential electrometry, a method for the measurement of electric charge translocation by membrane proteins. Developed by L.A. Drachev and co-workers, this method provides the time-resolved recording of light-induced electrical potential changes ($\Delta\Psi$) across a lipid-coated thin

collodion film with proteoliposomes adhered to one side of the film. The amplitude of $\Delta\Psi$ across the film changes proportionally to that on the proteoliposomal membrane, thus allowing the kinetics of charge translocation to be followed. This method, referred also as capacitive coupling [37], was applied originally for the studies of BR [38–40]. An alternative approach involved measurements of photocurrents from purple membrane oriented in films and gels (reviewed in [41]). The electrometric techniques were successfully used to study bacterial reaction centers [42,43], chromatophores [44,45], pigment-protein complexes of photosystems 2 and 1 [46,47], cytochrome oxidase [48–52] and recently a sodium pump [53].

For BR, it was found that photoelectrical potential $\Delta\Psi$ includes three main well-defined phases. Photoisomerization of the chromophore and subsequent relaxation of the retinal binding site during the BR \rightarrow K \rightarrow L transitions result in a small (ca. 5%) negative phase of $\Delta\Psi$. Subsequent proton transfer from the Schiff base to Asp85 and almost simultaneous proton release during the L \rightarrow M transition are accompanied by a positive microsecond phase (ca. 70 μ s). Reprotonation of the Schiff base, followed by proton uptake, reisomerization of the chromophore and deprotonation of Asp85 in the M \leftrightarrow N \leftrightarrow O \rightarrow BR transitions comprise the four times larger in magnitude millisecond (ca. 10 ms) phase [54,55]. More recent studies of light-induced electrogenic responses from eubacterial proteorhodopsin [56,57] and the pH dependence of H⁺ transport by this protein [35] showed that they correlate with the highly elevated pK_a of the counterion in that protein. In experiments with oocytes containing *Gloeobacter* rhodopsin the influence of pH and the membrane electrochemical gradient on the amplitude and direction of the photocurrents were examined [58].

In this work, we examined the mechanism of charge transfer in ESR reconstituted into phospholipid vesicles using time-resolved electrometry and optical absorption spectroscopy. The data obtained show that the electrogenic phases of light-driven proton transfer by ESR correlate with the optically detected transitions in the photocycle. The kinetics of the main steps of intramembrane proton transfer and its pH dependence differ significantly from that of BR, reflecting different proton donor and altered proton uptake and release mechanisms.

2. Materials and methods

2.1. Materials

ESR was expressed in *E. coli* BL21 (DE3)pLysS and purified according to [24]. For preparation of proteoliposomes the protein was solubilized in OG from Anatrace (USA). Other chemicals were from Sigma and Panreac (Spain).

2.2. Reconstitution of ESR into phospholipid liposomes

Liposomes were produced from azolectin (20 mg/ml Sigma, type IV-S, 40% w/w phosphatidylcholine content) by sonication (at 22 kHz, 60 μ A) for 2 min in 1 ml of 25 mM HEPES-NaOH buffer, pH 7.5. Reconstitution of ESR into proteoliposomes was carried out by mixing the liposomes with ESR in 1.5% (w/v) OG at the lipid/protein ratio of 100:1 (w/w) for 30 min in the dark. Removal of detergent was performed according to [59] using Bio-Beads SM-2 adsorbent (Bio-Rad). The detergent was removed by addition of a 20-fold excess of Bio-Beads (by weight) and stirring the suspension for 3 h at room temperature. The proteoliposomes were separated from Bio-Beads® by decanting. The proteoliposome suspension was pelleted at 140,000g at 4 °C for 1 h in a Beckman L-90K ultracentrifuge. The pellet was resuspended in 25 mM MES-NaOH (pH 6.5) buffer. Similar to proteorhodopsin [60], reconstitution of ESR into liposomes occurred with high degree of unidirectional orientation, as previous measurements of light-induced pH changes indicated [30], and large light-induced potential changes observed in this study.

2.3. Spectroscopic characterization

Flash-induced absorption changes of ESR in suspension of proteoliposomes were examined with lab-made flash-photolysis system similar to that described in [30]. Prior to measurements, all samples were adjusted to $A_{530} = 0.1$. Flash (532 nm, 8 ns, 10 mJ) was from LS-2131M Nd-YAG Q-switched laser (LOTIS TII, Belarus). Transient absorption changes were detected by photomultiplier and digitized by Octopus CompuScope 8327 (GaGe, Canada). The kinetic traces were fit with a sum of exponentials using Mathematica (Wolfram Research, USA).

2.4. Electrometric time-resolved measurements of the membrane potential generation

Generation of the transmembrane electric potential difference $\Delta\Psi$ was studied using a direct electrometric setup with time resolution of 100 ns as described in [38,39]. This technique includes fusion of the proteoliposomes with the surface of a collodion phospholipid-impregnated film (a membrane) separating two sections of the measuring cell filled with a buffer solution. The membrane should be thin enough and possess large electric capacitance (about 5 nF) for detecting fast charge translocation events. A pulsed Nd-YAG laser (YG-481, Quantel, $\lambda = 532$ nm, pulse half-width 12 nsec, flash energy up to 40 mJ) was used as a source of flashes. In the process of the light-driven proton transfer, ESR creates $\Delta\Psi$ across the vesicle membrane, which is proportionately divided with the measuring membrane and thus can be detected by Ag^+/AgCl electrodes immersed in a solution at different sides of the membrane. Typically, the measuring membrane has high resistance of 2–3 GOhm, and the light-induced $\Delta\Psi$ decays with a time constant of several seconds at neutral and high pH. A mix of 10 mM MES/Hepes/Tris/Ches was used for maintaining the pH in the range between pH 5 and 9.5. Typically, 15–30 min were required for equilibration after changing pH by a small amount of NaOH or HCl.

2.5. Electrometric data analysis

In order to obtain the rate constants and intrinsic amplitudes of the electrogenic events coupled to the corresponding transitions in the photocycle of ESR, the photoelectric traces were analyzed with two methods. According to the first method, the traces were fitted similar to the optical data as a sum of exponential terms (starting from zero time) in a similar way as it has been done initially for the photoelectric responses of bacteriorhodopsin and cytochrome oxidase [39,48,49,54,55,61–63]. The deconvolution of the overall multiphasic electrogenic response into individual exponentials gives true time constants of the phases, whereas the interpretation of the relative amplitudes will depend on the kinetic model employed [64,65].

If the electrogenic phases are related to parallel processes, then the intrinsic amplitudes of the electrogenic steps are simply equal to those found by deconvolution of the electrometric curves. This is not the case if the individual electrogenic phases are associated with consecutive processes. The relative amplitudes are especially affected when the rates of the electrogenic processes differ by less than one order of magnitude [64]. Theoretically, the true amplitudes of the electrogenic events corresponding to the model of consecutive steps of the photocycle can be obtained from the observed amplitudes by recalculating with the algebraic equations [64–66]. To obtain the intrinsic amplitudes empirically, we employed the method developed initially by Verkhovsky group to fit the electrometric curve directly with the sequential reaction model [50,67–69].

The kinetic curves were processed and deconvoluted into exponentials using program packages Pluk [70], Origin (OriginLab Corporation, USA) and MATLAB (The Mathworks, South Natick, MA). To fit experimental data by a sequential reaction model, the MATLAB was used.

3. Results

The kinetics of light-induced changes of transmembrane potential difference $\Delta\Psi$ from ESR containing proteoliposomes attached to a collodion film were examined at several pH values between pH 5.1 and 9.5 (Fig. 1) in parallel with measurements of the absorption changes of proteoliposomes at selected wavelengths, as described below.

3.1. ESR electrogenic response and photocycle at neutral pH

Upon laser flash, a photoelectric response of ESR-containing proteoliposomes adsorbed onto the lipid-impregnated collodion film ($\Delta\Psi$) was recorded in microsecond and millisecond time range. The sign of the $\Delta\Psi$ corresponds to the transfer of a positive charge from the interior of the proteoliposomes to the external bulk phase. The flash-induced photopotential increases up to ~30 mV, then it is followed by a passive discharge of the membrane and return of the electric potential to the initial level on the time scale of several seconds (Fig. 1A and B). The typical amplitude of $\Delta\Psi$ varied in different experiments in the range between 20 and 40 mV, depending on the efficiency of proteoliposome association with the measuring membrane.

In order to compare the electrical events with reactions of the photocycle, the kinetics of light-induced absorption changes in the ESR proteoliposomes were recorded at four characteristic wavelengths (Fig. 2A). The unresolved changes of absorbance upon the flash at the 590 nm and 510 nm reflect formation of the K intermediate and bleach of the absorption band of ESR in the initial state (see Fig. S1). The decay of the K intermediate occurring on the microsecond time scale are accompanied by decrease of absorption at 590 nm, 550 nm and 510 nm. This is followed by the increase of absorption at 410 nm, which reflects accumulation of the M intermediate upon Schiff base deprotonation and transfer of a proton to the proton acceptor Asp85. Inflection at 510 nm apparently indicates formation of L, however L does not accumulate in large amount in ESR, apparently from equilibrium being shifted from L to K and M [30,31]. The subsequent decrease of absorption at 410 nm and concurrent increase at 550 nm and 510 nm reflect the decay of the M state and formation of the N1 intermediate upon reprotonation of the Schiff base (Fig. 2A). This transition ($M \leftrightarrow N1$) is characterized by the increase of absorption with a maximum at 550 nm and a minimum at 400 nm [30]. The following transition ($N1 \leftrightarrow N2/O$) is characterized by the increase of absorption with a maximum at 590 nm. Decay of the N2/O state and recovery of the initial state of ESR results in the decrease of absorption at 590 nm and concurrent increase at 510 nm, correspondingly (Fig. 2A). To obtain the characteristic time constants the traces were fitted globally (summarized in Table 1). The parameters of the spectroscopic measurements were analyzed in comparison with time constants and amplitudes of the corresponding electrogenic phases.

The photoelectric response was fitted with a sum of individual exponential terms ($\sum A_i e^{-t/\tau_i} + \text{const}$) and by the sequential reaction model, which yields more accurate amplitudes of the kinetic components of $\Delta\Psi$ (see Material and methods). Five positive components of $\Delta\Psi$ generation with similar time constants (Table 1) were revealed with both data treatments (Fig. S2).

The two fastest components of generation of $\Delta\Psi$ (~3 μs and ~50 μs) presumably reflect electrogenic events associated with the deprotonation of the Schiff base, transfer of a proton to the primary proton acceptor Asp85 and formation of the M intermediate. This assumption is supported by the light-induced increase of absorption at 410 nm, which develops simultaneously and is characterized by two similar rate constants, ~4.9 μs and ~60 μs (Table 1). The overall amplitude of these electrogenic events constitutes ~4.5% of the total photoresponse.

Thereafter, the absorption at 410 nm decreases with $\tau \sim 0.4$ ms with concurrent increase in absorption at 550 nm presumably from the decay of the M state and appearance of the N1 intermediate. In the kinetics of $\Delta\Psi$ this process corresponds to the third electrogenic phase (with

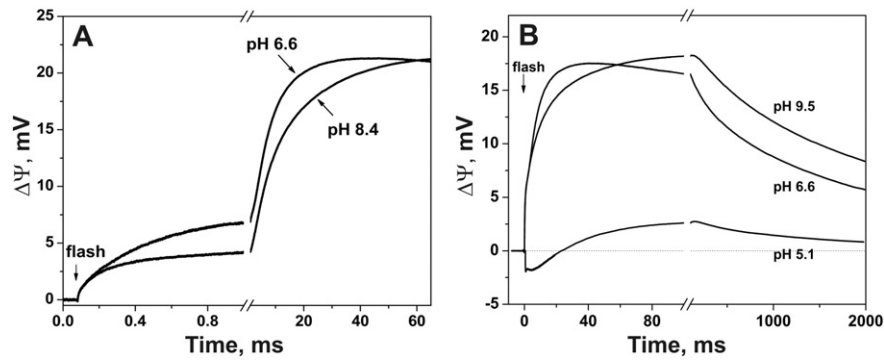


Fig. 1. A) Comparison of the kinetics of transmembrane electric potential difference generation $\Delta\Psi$ by ESR at pH 6.6 and pH 8.4. The curves are normalized by the amplitude. B) Generation of transmembrane electric potential difference $\Delta\Psi$ by ESR at different pH.

$\tau \sim 0.5$ ms), which makes a large contribution to the overall photoelectric response ($\sim 35\%$). This component reflects mostly an uptake of a proton at the cytoplasmic surface of the protein and its transfer through the cytoplasmic channel to the Schiff base during the M to N1 transition.

The subsequent transition, which involves an increase of absorption at 590 nm, has a rate constant of ~ 4.7 ms; it corresponds to the formation of the N2/O intermediate [30]. It is accompanied by the minor absorbance decrease at 410 nm from the decay of a small fraction of the M state to the N1 and the N2/O intermediates. According to the FTIR data, at the end of the photocycle the chromophore in ESR is still mostly in the 13-*cis* configuration, characteristic for the N state, however some fraction of the retinal chromophore with *trans* configuration, characteristic for the O-like state, is also present [31]. Hence, we use N2/O notation for this mixture of states. The N1 \leftrightarrow N2/O transition makes similar contribution to the electrogenicity ($\sim 37\%$) to that of the M \leftrightarrow N1 transition. The N2 state is more red shifted compared to N1 and has a higher pK_a of the Schiff base [32] as follows from the shift of the equilibrium from M to N2.

The next electrogenic component with $\tau \sim 14$ ms contributes 21% of the total photoelectric response. It coincides with the decrease of absorption at 590 nm and increase of the absorption at 510 nm, which represent the decay of the N2/O state to the initial state in the N2/O \rightarrow ESR transition with $\tau \sim 17$ ms. The associated electrogenic event reflects the release of a proton to the bulk phase from the Asp85-His57 site [33] through currently unidentified residue or a group of residues in the extracellular domain.

3.2. ESR photocycle and electrogenic response at alkaline pH

Measurement of the flash-induced photoelectric response at alkaline pH (pH 8.4) and its comparison with that at pH 6.6 demonstrated that whereas the overall amplitudes of the photo-induced electric potential $\Delta\Psi$ are similar (Fig. 1A), its components associated with the

reprotonation of the Schiff base (the M decay) are significantly slower at pH 8.4 (Fig. 2B). Similar to pH 6.6, the increase of absorption at 410 nm is biphasic (~ 6 μ s and ~ 52 μ s); but the amplitude (amount of the M intermediate) is substantially larger (Fig. 2B). These absorption changes correlate with two phases of $\Delta\Psi$ (~ 3 μ s and ~ 48 μ s), contributing in sum about 6% of the total photoelectric response, 1.5 fold more than at pH 6.6 (Table 1).

Three subsequent electrogenic components make the major contribution to the $\Delta\Psi$ at pH 8.4: ~ 0.23 ms ($\sim 11\%$), 4.5 ms ($\sim 31\%$) and 23 ms ($\sim 51\%$). The sequential model gives the following rate constants and amplitudes for the transitions in the millisecond time range: 0.3 ms ($\sim 8\%$), 4.7 ms ($\sim 44\%$) and 24.9 ms ($\sim 37\%$). The theoretical curves and residuals of the fits are shown in Fig. S3.

The global fit of the absorbance changes revealed three transitions in the submillisecond-millisecond time domain at pH 8.4 (~ 0.7 ms, ~ 3 ms and ~ 19 ms). The rate constants of these transitions are similar to those at neutral pH but unlike at pH 6.6, the changes of absorbance at 410 nm, 510 nm and 550 nm at pH 8.4, assigned to the ~ 0.7 ms transition, correspond to a small increase of the amount of the M intermediate rather than decrease, in agreement with the previous observation of the slow phases of the M rise at high pH in ESR [32]. Notably, the decay of the M intermediate at alkaline pH occurs significantly slower than at pH 6.6 (~ 3 ms vs ~ 0.5 ms). Correspondingly, the increase of absorption at 550 nm, due to the formation of the N1 state, is also significantly slower (Fig. 2B). It coincides with the decay of the M intermediate at 410 nm and, at the same time, with the increase of absorption at 590 nm. The last one reflects formation of the N2/O intermediate.

One can conclude that at pH 8.4 the M intermediate transforms to the N2/O state in the course of the 3 ms transition, without significant accumulation of the N1 intermediate. Therefore, the increase of pH results in the change of the relative contributions of the two components of the M intermediate decay. These results are in accord with the previous study of ESR solubilized in lipid-like detergent, which

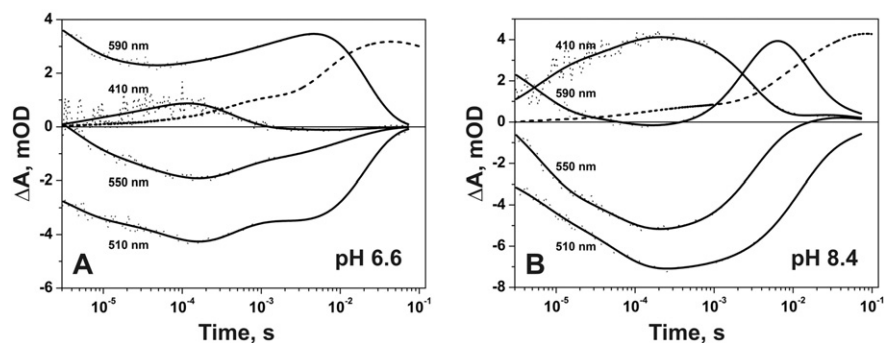


Fig. 2. Light-induced absorbance changes in suspension of proteoliposomes at pH 6.6 (A) and pH 8.4 (B). Traces at four characteristic wavelengths (410, 510, 550, 590 nm) are shown. Dashed lines, changes of the electrical potential ($\Delta\Psi$) in arbitrary units.

Table 1

Time constants and amplitudes of potential generation and associated changes of absorbance upon charge translocation during the photocycle of ESR.

pH	Electrogenic phases				Changes of absorbance ^a		
	Fit by sum of exponential terms		Fit by sequential reaction model		τ , ms	at 410 nm, mOD	at 590 nm, mOD
	τ , ms	contribution, %	τ , ms	contribution, %			
6.6 ^b	0.0042	2.1	0.0039	3.3	0.0049	-0.4	2.3
	0.032	1.1	0.026	3.2	0.061	-1.1	0.2
	0.58	37	0.502	35	0.4	1.4	-0.6
	4.87	38	3.51	37	4.7	0.2	-3.3
	14.3	22	13.9	21	17.5	-0.23	6.1
8.4 ^b	0.0026	1.8	0.0045	2.4	0.0056	-2.6	3.1
	0.048	4.3	0.0689	7.8	0.052	-1.7	0.8
	0.23	11	0.301	8.3	0.71	-1	1.8
	4.51	31	4.73	44	2.7	5.3	-10
	23.5	51	24.91	37	19	-0.1	7.1
5.1 ^c	0.001	-18	N/A ^d		0.0089	-1.06	1.9
	0.032	-5	N/A		0.029	1.38	-1
	0.14	-22	N/A		0.13	-0.69	-0.7
	3.5	-55	N/A		9.5	0.26	-7.9
	0.36	25	N/A		0.50	0.03	2.9
	38	75	N/A		16.2	-0.43	9

^a To obtain parameters of spectroscopic measurements (time constants and amplitudes), the changes of absorbance at four characteristic wavelengths (410, 510, 550, 590 nm) were fitted globally.

^b For the electrometric traces at pH 6.6 and pH 8.4, to obtain a satisfactory fit by the sum of exponential terms, $\sum A_i [1 - \exp(-t/\tau_i)]$, we had to include a negative component with a time constant of ~ 1.3 ms; for the fit by the sequential reaction model the phase with missing contribution to the electrogenicity is not shown in the table.

^c Negative and positive electrogenic components are grouped.

^d N/A – non-applicable (fit was done only with a sum of exponential terms).

showed that in the pH region between 7 and 9 fraction of the faster component of the M decay decreases from 80% to 0% with $pK_a = 8.1$ [32]. Similarly to that at pH 6.6, the final transition of the ESR photocycle at alkaline pH is represented by decrease of the absorption at 590 nm and increase at 510 nm. These events reflect the decay of the N2/O intermediate and return to the initial state of ESR. This transition can be fitted by a single component with $\tau \sim 19$ ms, which is similar to the last phase of $\Delta\Psi$ generation (~ 23 ms).

At alkaline pH, we did not observe the ~ 0.5 ms electrogenic phase, which was responsible for the major part of $\Delta\Psi$ generation at pH 6.6 and was assigned to the $M \leftrightarrow N1$ transition. Instead, two electrogenic phases with $\tau \sim 0.25$ ms and $\tau \sim 4.5$ ms were resolved. The phase with $\tau \sim 0.25$ ms and a relative amplitude ~ 8 –11% was not detected in the parallel spectroscopic measurements, while the second one ($\tau \sim 4.5$ ms) contributed about 44% of the total $\Delta\Psi$ generation and coincided with the spectroscopically detected decay of the M state and formation of the N2/O intermediate ($M \leftrightarrow N2/O$ transition).

Thus, the increase of pH to 8.4 results in ca. 6–8-fold deceleration of the corresponding electrogenic process coupled to the M state decay. The final electrogenic component (~ 23 ms) corresponds in time to the decrease of absorption at 590 nm associated with the $N2/O \rightarrow ESR$ transition. It reflects the release of a proton from the primary acceptor Asp85 to the bulk phase, making about 37% contribution to the overall photoelectric response. From the optical data, it is evident that the transitions $M \leftrightarrow N2/O \rightarrow ESR$ represent the consecutive events in the photocycle of ESR with the rate constants that differ by less than an order of magnitude. That is why (see Materials and methods for details), the accurate values of the amplitudes for the corresponding electrogenic phases were obtained from the fit with the sequential reaction model (44% and 37%, respectively).

Increase of pH to 9.5 causes additional deceleration of the M decay and of the electric phases related to reprotonation of the Schiff base to 7.8 ms (Fig. 3). Capturing protons becomes the rate limiting step and slows all subsequent reactions. However, the overall amplitude of the photoelectric response at pH 9.5 remains large (Fig. 1B). We did not notice any substantial decrease or reversal of the potential observed for proteorhodopsin at high pH in a recent study [71]. The slowing of the optical and electrical signals associated with the M decay at high pH correlates with the observation that proton uptake from the bulk occurs during the M to N transition in ESR [32] rather than the N to O transition, as in BR [4,9,72].

3.3. ESR photocycle and electrogenic response at acidic pH

The light-induced changes of the photoelectric potential generated by ESR at pH 5.1 in response to a laser flash are shown in Fig. 4A. The main effect of acidification on the kinetics of $\Delta\Psi$ generation is a dramatic decrease of the overall amplitude of the response (by >10 fold). Furthermore, during the time range of several milliseconds, the response is negative, which corresponds to the transfer of a positive charge to the internal volume of proteoliposomes. Only at a later time ($\tau > 20$ ms) $\Delta\Psi$ is positive.

The kinetic phases of $\Delta\Psi$ with a negative sign have time constants of ~ 1 μ s, ~ 32 μ s, 0.14 ms and 3.5–4 ms (Table 1). They are superimposed with two positive phases (0.36 ms and 38 ms), the direction of which coincides with that of electrogenic phases at neutral and alkaline pH, i.e. corresponding to a positive charge movement out of the proteoliposomes. These phases are followed by a passive discharge of the membrane within several hundreds of milliseconds, which is significantly faster than at neutral pH. Thus, the electrical response at pH 5.1

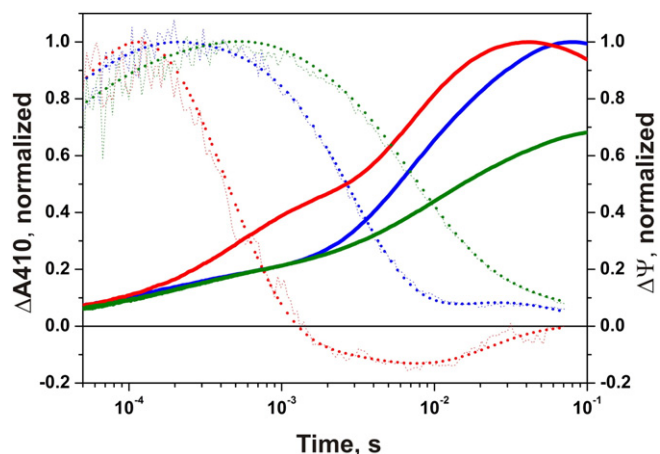


Fig. 3. Comparison of the kinetics of absorption changes at 410 nm (dotted lines) from the formation and decay of the M intermediate with the kinetics of $\Delta\Psi$ generation (straight lines) at pH 6.6 (red), pH 8.4 (blue) and 9.5 (green). The curves are normalized by the amplitude.

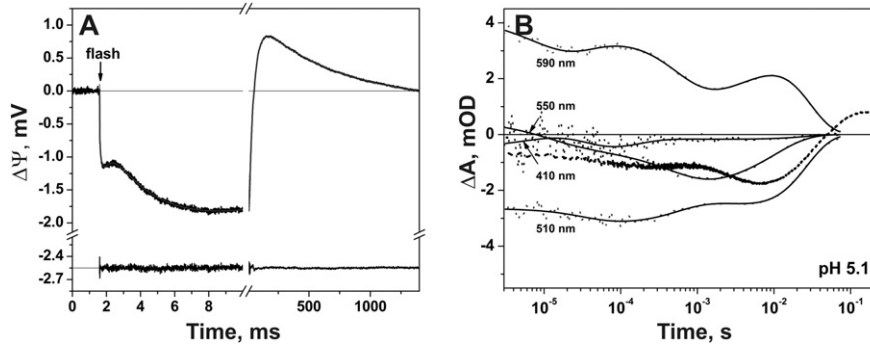


Fig. 4. A) Generation of transmembrane electric potential difference $\Delta\Psi$ by ESR at pH 5.1. The upper trace shows the experimental trace together with the fit (parameters are given in Table 1). The residuals are shown below. B) Absorbance changes during the photocycle of ESR at pH 5.1 at four wavelengths (410 nm, 510 nm, 550 nm, 590 nm). Dashed line is the change in electrical potential ($\Delta\Psi$) in arbitrary units.

exhibits substantial negative phases and dramatically decreased and slowed positive components. The latter indicates that at pH 5.1, despite the apparent absence of the M intermediate accumulation some fraction of ESR pumps protons in a single-turnover regime from the internal volume of proteoliposome to the output phase, in the same direction as at pH 8.4 and 6.6. The sum of the amplitudes of the positive phases exceeds the total amplitude of negative phases at pH 5.1 by 1 mV, which constitutes 4–5% of the total amplitude at pH 8.4.

The corresponding light-induced absorbance changes are shown in Fig. 4B. Their global fit revealed 6 transitions (Table 1). The typical absorbance decrease, which corresponds to the decay of the K/L intermediates in the initial part of the ESR photocycle, is characterized by the two fastest rate constants ($\sim 8.9 \mu\text{s}$ and $\sim 28 \mu\text{s}$), which are similar to the values obtained at pH 6.6 and 8.4. Noteworthy, at pH 5.1 no significant absorbance changes at 410 nm were observed. As it was proposed earlier [32], the M intermediate is not accumulated to a considerable level at this pH presumably because of the decreased yield and formation rate, and probably relatively fast decay into the following intermediates of the photocycle.

In contrast to neutral and alkaline pH, the absorbance increase at 590 nm includes two components at pH 5.1 (Fig. 4B). The rapid component occurs with rate constant of $\sim 0.13 \text{ ms}$. It is followed by the decrease of absorbance with the rate constant of $\sim 0.5 \text{ ms}$ and concurrent increase of absorbance at 510 nm. These absorbance changes resemble those at high pH, which are associated with the formation of the N2 and subsequent decay of the N2/O intermediate to the initial state of ESR, but with faster rate constants. The slowest component, with the time constant of 0.5 ms, correlates with a small positive current, which might be attributed to a small fraction of pigment which pumps protons fast at this pH.

The slower phase of the absorbance increase at 590 nm is characterized by the rate constant of 8–9 ms. It is not accompanied by the change of absorbance at 510 nm, which is typical for the formation of the N2/O state from the N1 state at neutral pH (the slow component of the

formation of the state with the reprotonated Schiff base). At pH 5.1, we have not detected the absorbance changes at 410 nm and 550 nm, which correspond to the $M \leftrightarrow N1$ transition. The following decrease of absorption at 590 nm with the time constant $\sim 16 \text{ ms}$ in parallel with increase of absorption at 510 nm can be interpreted as the $N2/O \rightarrow \text{ESR}$ transition. It roughly corresponds to the $\sim 38 \text{ ms}$ electrogenic phase.

3.4. Fast negative electrogenic phase precedes formation of the M state at high pH

At the first sight, the fast negative electrogenic phase, which is characteristic for the early stage of the photoelectric response of BR [55], is absent in ESR at neutral and high pH. But an accurate analysis revealed that this is not true. By the comparison of the photoelectric kinetics of ESR at three different pH values (Fig. 5) one can observe that the early parts of the kinetics at pH 8.4, 6.6 and 5.1 are similar in the initial 0.2–0.3 μs and the direction of these phases is negative. But later the kinetics at alkaline and neutral pH are significantly different from that at the acidic pH. It is evident that at pH 6.6 and pH 8.4, the negative electrogenic phase is superimposed with the large positive electrogenic phases with rate constants of several microseconds. These positive electrogenic phases reflect proton transfer from the Schiff base to the Asp85 during the M state formation in ESR. At acidic pH, they are absent or small in amplitude, and, as a result, mostly the pure negative electrogenic phase corresponding to the $K \rightarrow L$ transition is observed.

Assuming that the primary events during the early stages of the photocycle ($\text{ESR} \rightarrow K \rightarrow L$) are accompanied by similar electrogenic events at low and high pH, we subtracted the kinetics at pH 5.1 from that at pH 6.6 (Fig. 5B), and obtained the kinetics of the electrogenic phases, which correspond to the $L \rightarrow M$ transition ($\sim 3 \mu\text{s}$ and $\sim 40 \mu\text{s}$). The overall amplitude of these phases constitutes $\sim 9\%$ of the total photoelectric response. This is consistent with the value, which one can expect from the distance between the Schiff base and the proton

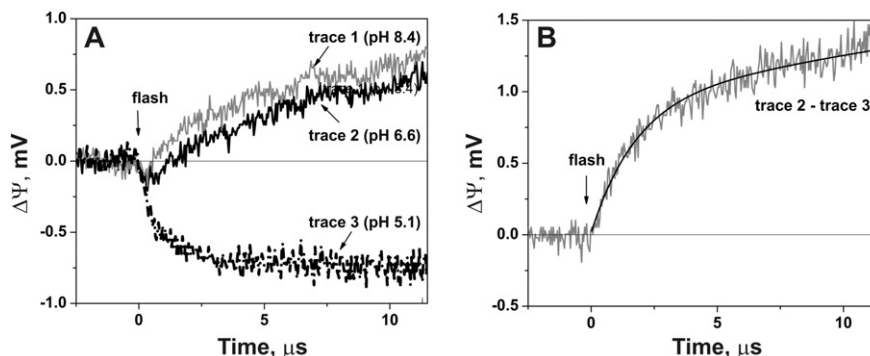


Fig. 5. Kinetics of the photo-induced electric potential generation by ESR in the microsecond time scale at pH 8.4, 6.6, 5.1 (A). B - the trace at pH 5.1 is subtracted from the trace at pH 6.6.

acceptor residue Asp85 in ESR ($4 \text{ \AA} \sim 1/10$ of the membrane thickness) [33]. Noteworthy, in contrast to BR, the relative amplitude of the microsecond electrogenic phases is about 3 times smaller than the 50 μs component in BR, where this phase includes also the release of a proton from the PRG to the bulk [73,74].

4. Discussion

In this work we have resolved the kinetics of the light-induced membrane potential generation by ESR under single turnover excitation. The maximum amplitude of the photoelectric potential generated by ESR incorporated into the proteoliposomes that were obtained in our experiments was comparable to that of bacteriorhodopsin from *H. salinarum* [75]. However, the rate constants and relative amplitudes of the kinetic components of $\Delta\Psi$ generated by ESR exhibit significant differences from those of BR, consistent with the differences in proton transfer reactions between these proteins [24,30,32]. We have found that the negative electrogenic phase associated with the early stages of the BR photocycle (formation of the K and L intermediates) is also present in ESR. The next phase, which corresponds to deprotonation of the Schiff base (the M state formation), is smaller than in BR because it lacks contribution from proton release to the bulk, which is delayed in ESR to the end of the photocycle [24]. Other specific features of $\Delta\Psi$ generation by ESR related to its unique proton donor (Lys96 vs Asp96 in BR) are discussed below in comparison with those in BR.

4.1. Reprotonation of the Schiff base. Effect of pH on decay of the M intermediate and $\Delta\Psi$

Two electrogenic phases contribute mostly to the kinetics of $\Delta\Psi$ generation by BR (Fig. 6A, [39,55]). The first one is the proton transfer from the Schiff base to Asp85, concurrent with release of a proton from the proton release complex (PRG) to the extracellular surface ($\sim 50 \mu\text{s}$, 30%; Fig. 6A). The second one ($\sim 5\text{--}20 \text{ ms}$, 70%) involves proton transfer from the cytoplasmic surface to the Schiff base plus proton transfer from Asp85 to the PRG, for review see [9,40,41,55]. These electrogenic components correlate with the rise and decay of the M intermediate, respectively (Fig. 6A).

In ESR, the largest contribution to $\Delta\Psi$ at pH 6.6 is from $\sim 0.5 \text{ ms}$ and 4.5 ms electrogenic phases (72% total). These phases correlate with the kinetics of absorbance changes accompanying the $M \leftrightarrow N1 \rightarrow N2/O$ transitions, reflecting primarily the proton transfer from the bulk to the Schiff base and possibly reisomerization of a fraction of the chromophore from 13-*cis* to all-*trans* in the O intermediate (Table 1). The two phases (0.5 ms and 4.5 ms) at pH 6.6 probably originate from the reversibility of the $M \leftrightarrow N1$ transition and the contribution from the subsequent $N1 \rightarrow N2/O$ transition [32]. At pH 8.4, the corresponding electrogenic phase, coupled to the decay of the M state and generation of the N2/O state develops solely with the time constant of $\sim 4.5 \text{ ms}$ (Fig. 2B, Table 1).

In contrast to BR, the slowest electrogenic phase in ESR ($\sim 17 \text{ ms}$, pH 6.6) contributes much less ($\sim 22\%$) to the photoelectric response. It corresponds to the $N2/O \rightarrow \text{ESR}$ transition and is caused mostly by deprotonation of Asp85 and release of a proton to the bulk.

The main effect of the increase of pH on the kinetics of ESR photocycle is the significant deceleration of the M decay and coupled charge transfer reaction. The prime reason for it is that proton uptake from the bulk occurs during the lifetime of the M intermediate (in the $M1 \leftrightarrow M2$ transition) and precedes reprotonation of the Schiff base [32]. This is different from BR, in which the $M \leftrightarrow N1$ transition involves internal proton transport from Asp96 to the Schiff base and hence does not depend on pH, while the next transition, $N1 \leftrightarrow N2/O$ [9] is pH dependent because during this transition proton uptake takes place leading to reprotonation of Asp96, with pK_a 7.2–7.5 [72,76]. In contrast to BR, the proton donor to the Schiff base in ESR is unprotonated in the initial state; its pK_a is elevated in the photocycle reaching the value 8.1–8.6 in the M state [32].

The pH dependence of the Schiff base reprotonation in ESR is presumably determined by the pK_a of the donor and/or of the Schiff base in the $M \leftrightarrow N1 \leftrightarrow N2$ transitions [32]. Interestingly, the pK_a of the Schiff base of BR in the M to N transition was estimated to be 8.2–8.3 under condition when donor was removed by the D96N mutation and proton delivery was assisted by addition of sodium azide [77].

4.2. On the relative amplitudes of the electrogenic phases corresponding to Schiff base protonation, counterion deprotonation, and donor protonation in ESR

The two fastest electrogenic stages associated with the $L \rightarrow M$ transition of photocycle ($\sim 3 \mu\text{s}$ and $\sim 40 \mu\text{s}$) contribute $\sim 9\%$ to the

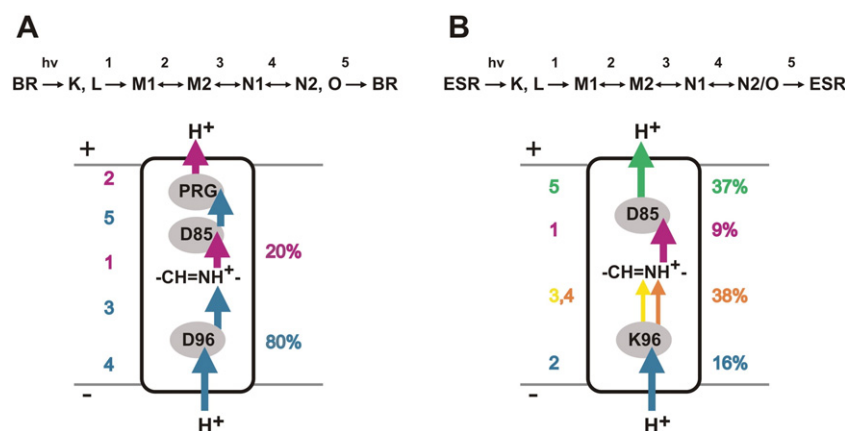


Fig. 6. A. The photocycle transitions (top line) and major electrogenic steps (1 through 5) coupled to proton transfer in BR (bottom). 1 (purple arrow), proton translocation from the Schiff base to the primary acceptor Asp85; 2 (purple arrow), release of a proton from the PRG (proton release group) to the outer surface; 3 (blue arrow), transfer of a proton from Asp96 to the Schiff base; 4 (blue arrow), transfer from the cytoplasmic surface to Asp96; 5 (blue arrow), transfer of a proton from Asp85 to the PRG. For BR, steps 1 and 2 are related to the microsecond (ca. 100 μs) phase and in sum comprise 20% of total response, whereas steps 3, 4 and 5 occur during millisecond (2–10 ms) phase of membrane potential generation, which comprises 80% [54]. B. The photocycle transitions (top line) and major electrogenic steps (1 through 5) coupled to proton transfer in ESR (bottom). 1 (purple arrow), proton translocation from the Schiff base to the primary acceptor D85; 2 (blue arrow), transfer of a proton from the cytoplasmic surface to Lys96; 3, 4 (yellow and brown arrows), transfer of a proton from Lys96 to the Schiff base; 5 (green arrow), release of a proton from the primary acceptor to the outer surface. The thickness of the arrows corresponds to the fraction of transferred protons in a transition. Tentative contribution of each step to overall amplitude of $\Delta\Psi$ is given in percents on the right. The principal distinction of the proton-motive mechanism of ESR is that step 2 involves proton uptake and presumably protonation of Lys96, whereas in BR step 2 reflects proton release to the outer phase from the PRG. The second difference is that the final step of the photocycle in ESR (step 5) involves release of a proton to the outer phase from Asp85, whereas in BR it involves internal transfer from Asp85 to the PRG [9,76].

photoelectric response (Fig. 6B, step 1). The apparent amplitude of the electrogenic phase assigned to the decay of the M state is significantly smaller at alkaline pH than at neutral pH (44% vs 72%). This difference probably is related to the finding that the photoelectric response at pH 8.4 includes additional electrogenic component with $\tau \sim 0.25$ – 0.3 ms comprising about 8–11% of the total response. There were no corresponding absorbance changes found, hence the electrogenic process with $\tau \sim 0.25$ – 0.3 ms is likely to reflect an optically silent event, the protonation of the internal proton donor (Lys96) from the cytoplasmic side in the M1 \leftrightarrow M2 transition (Fig. 6B, step 2) [32]. If so, then the following electrogenic component at pH 8.4 ($\tau \sim 4.5$ ms) results from the proton transfer from Lys96 to the Schiff base (Fig. 6B, steps 3 and 4).

At pH 6.6, the proton transfer to Lys96 occurs almost simultaneously with the proton transfer to the Schiff base [32] (0.5 ms in our study, Fig. 6B, steps 2 and 3), whereas at pH 8.4 the latter one is about 10 times delayed (Fig. 6B, step 4). A possible explanation for the slower reprotonation of the Schiff base at pH 8.4 than at pH 6.6 is that only a fraction of donor and the Schiff base can be protonated fast at high pH. Presumably, the pK_a of the donor and the Schiff base in the M \leftrightarrow N1 is higher than 6.6, therefore a large fraction (>0.5) of the Schiff base is protonated within the fast phase at pH 6.6 (Fig. 6B, steps 2 and 3). At pH 8.4, only a small fraction of N1 accumulates, which converts slowly to N2/O. The latter state presumably has a higher pK_a of the Schiff base, so the rate of the N1 \leftrightarrow N2/O transition would determine the kinetics of the Schiff base reprotonation, until the rate of proton uptake becomes rate limiting at pH > 9 [32].

Thus, electrogenic protonation of Lys96 can be detected as a separate phase because of significant deceleration of the proton transfer from Lys96 to the Schiff base at alkaline pH. The relative amplitude (~ 8 – 11%) of the 0.25 ms electrogenic phase at pH 8.4 corresponds to the distance of Lys96 from the internal water phase, which can be estimated as $\sim 1/10$ of the membrane thickness. However, one should take into account that if the pK_a of Lys96 in the M state is ca 8.6, only part of this residue could be in the protonated state. As a result, the amplitude of the corresponding electrogenic phase could reflect protonation of Lys96 only in a fraction of ESR (ca. 50% assuming pK_a 8.6 [32]) and therefore the relative contribution of the electrogenic transfer of a proton from cytoplasm to Lys96 should be approximately doubled (to ca 16%; see Fig. 6B, step 2). Accordingly, the electrogenicity of the proton transfer from Lys96 to the Schiff Base ($\sim 38\%$; Fig. 6B, steps 3 and 4) is slightly less than the amplitude of the 4.5 ms electrogenic phase ($\sim 44\%$), which includes not only protonation of the Schiff Base from Lys96, but also transfer of a proton to the unprotonated portion of the Lys96. So, from the amplitude of the $\Delta\Psi$ phases coupled to the M decay, the electrogenic distance between the cytoplasmic side and the Schiff base is estimated at $\sim 54\%$ of the membrane dielectric thickness (Fig. 6B).

The amplitude of the slowest electrogenic phase, coupled to the N2/O \rightarrow ESR transition, is significantly smaller at pH 6.6 than at pH 8.4 (22% vs. 37%). The latter value (37%) correlates well with the distance from the Schiff base to the extracellular surface according to the available structural data for ESR [33] (Fig. 6B, step 5). This difference may indicate that the fraction of the protonated donor (Lys96) might be higher at neutral pH compared to that at alkaline pH during the M to N2 photocycle transition, and the donor might undergo deprotonation to the bulk during the last phase of the photocycle. The latter possibility suggests that Lys96 might be in the protonated state not only in M, when the Schiff base is deprotonated, but also later in the photocycle (in N2/O), and restores its neutral state only during the N2/O \rightarrow ESR transition. This does not imply a futile photocycle.

The photopotential generated at each stage of the process is directly proportional to the projection (r) of the pathway of the proton movement onto the normal to the membrane and inversely proportional to the dielectric constant (ϵ) of the membrane: $\sim kr/\epsilon$ [78]. The electrogenic and structural distances might not coincide since the photoelectric potential generated by the light-induced charge movements depends on

the local dielectric constant, which might not be homogeneous through the proton pathway in the protein and requires exact estimation of the projection of the distance onto the membrane normal. Moreover, reversible reactions complicate the precise estimation of the $\Delta\Psi$ components, which can be assigned to each transition.

Assuming that the thickness of the hydrophobic insulating layer of proteoliposomes is ~ 40 Å, and the dielectric constant is homogeneous, the electrogenic distances of the charge transfers (in projection, normal to the surface) could be estimated during reprotonation of the Schiff base and the release of proton from Asp85 to the extracellular side as $40 * 0.54 = 21.6$ Å and $40 * 0.37 = 14.8$ Å, respectively. The electrogenic distance between cytoplasmic phase and Lys96, and between Lys96 and the Schiff base is estimated as $40 * 0.16 = 6.5$ Å and $22 - 6.5 = 13.5$ Å, which is close to the distances obtained from the structural data [33] for the initial state.

4.3. The features of the kinetics of $\Delta\Psi$ generation coupled to the photocycle of ESR at pH 5.1

The photoelectric potential at pH 5.1 exhibits much smaller amplitude of positive phases in comparison with the responses at neutral and alkaline pH and the presence of larger negative phases. The positive phases can be attributed to the H^+ pumping cycle similar to the one observed at pH 6.6 and 8.4 though with a significantly smaller amplitude and much slower rise. Earlier measurements of the light-induced pH changes in the suspensions of *E. coli* cells and proteoliposomes demonstrated that ESR was capable of pumping at pH 5, though with less efficiency than at neutral pH [30]. A decrease in the amplitude of the positive electrogenic phases at acidic pH found in this study can be explained by the protonation of the primary proton acceptor Asp85 already in the initial state, however, actual titration of the protein in detergent (DDM) showed that only a fraction of it (20–30%) is protonated at pH 5.1 while complete protonation occurs below pH 3 [30]. The second factor affecting the kinetics and amplitude of positive phases is the close interaction of Asp85 with His57, as was revealed in crystallographic structure of ESR [33] and by mutating His57 [30]. It was suggested that protonation of His57 (with pK_a ca 6 in the lipid environment) decreases proton affinity of Asp85 and, hence, reduces accumulation and the rate of formation of the M intermediate at low pH [30,31]. On the other hand, at low pH reprotonation is expected to be fast, preventing detectable accumulation of M. This can account for the appearance of the slow ($\tau \sim 38$ ms) positive phase at pH 5.1 in the absence of accumulation of the M intermediate. This phase can be assigned to a slowly pumping photocycle in which the M formation is delayed due to the protonation of His57. A minor positive electrogenic phase with $\tau \sim 0.5$ ms might originate from a small fraction of the protein that functions in the same way as at pH 6.6.

The origin of the negative electrogenic phases (0.14 ms and ~ 3.5 – 4 ms) is not clear. Probably they are caused by relatively small charge movements in the protein rather than by a reverse proton transport or a leak. They are likely to be caused by the movements of protons in the direction opposite to normal proton transfer between ionizable residues. For instance, they might involve protonation of Asp85 from His57. It would cause a red shift of the spectrum and might explain an absorption increase at 590 nm, which occurs with $\tau \sim 0.13$ ms. Subsequent reprotonation of His57 from the extracellular side could also produce a negative current. A more precise understanding of the origin of these negative phases at low pH would require additional studies involving mutant proteins and other approaches.

5. Conclusions

In this work we have resolved the kinetics of membrane potential generation, $\Delta\Psi$, coupled to the photocycle transitions in ESR, including those which involve its unusual proton donor (Lys96). Several differences were found in kinetics, amplitude and pH dependence of

electrical components of $\Delta\Psi$ in ESR with those in best studied H⁺ pump, BR. In ESR, the electrogenic events accompanying the M decay (reprotonation of the Schiff base) are primarily pH dependent, whereas in BR it is the N decay, which is pH dependent. This difference originates from different initial protonation state of the donor to the Schiff base and reaction of the photocycle in which proton is taken up (these are M to N1 in ESR and N1 to N2 in BR). Other differences are caused by different mechanism of proton release in ESR and BR and counterion structure (presence of ionizable His57 close to Asp85 in ESR).

Formation of the M intermediate (upon Schiff base deprotonation) is associated with two positive electrogenic phases (~3 μ s and ~40 μ s) of $\Delta\Psi$ generation by ESR, which comprise ~9% of the total photoelectric response and correspond to the distance between the Schiff base and the primary proton acceptor Asp85. This is about 3 times less than the contribution of the 50 μ s component in BR, which includes also movement of Arg82 to the proton release group and release of a proton to the bulk. The subsequent electrogenic reprotonation of the Schiff base of ESR from the cytoplasmic side (M \leftrightarrow N1 \leftrightarrow N2/O transitions) occurs with $\tau \sim 0.5$ ms and 4.5 ms. At pH 8.4, the fast component ceases and the Schiff base reprotonation slows down, indicating that capturing a proton from the bulk becomes the rate limiting step.

At alkaline pH, a spectrally silent electrogenic component with $\tau \sim 0.25$ ms was detected, which can be attributed to the proton transfer from the bulk to primary donor of proton, Lys96 (in the M1 \leftrightarrow M2 transition). Proton release from Asp85 to the bulk in the N2/O \rightarrow ESR transition results in the slowest electrogenic component (~14 ms, pH 6.6). It is smaller than the millisecond component of $\Delta\Psi$ generation in BR, which involves several processes, the reprotonation of the Schiff base from the cytoplasmic side, reprotonation of the donor Asp96 and proton transfer from Asp85 to the proton-release group. The relative amplitudes of the electrogenic components resolved during the photocycle of ESR correlate with the distances between corresponding proton exchangeable groups in three-dimensional structure of the protein and are in line with the proposed mechanism of proton transfer. At pH 5, the amplitude of $\Delta\Psi$ generation by ESR decreases 10 fold, and positive phases are strongly delayed presumably from protonation of the primary proton acceptor of Asp85 and/or closely interacting with it His57 in the initial state.

Transparency document

The Transparency document associated with this article can be found, in online version.

Acknowledgements

This work was supported by the grants from RFBR 14-04-00499a, 15-04-05922a, 15-04-06266a, 14-04-00153a, Molecular and Cell Biology Program of Russian Academy of Sciences and the grant SS-8384.2016.4. The authors thank Dr. Janos K. Lanyi for helpful suggestions on the manuscript.

Appendix A. Supplementary data

Supplementary data to this article can be found online at <http://dx.doi.org/10.1016/j.bbabo.2016.08.004>.

References

- [1] J.L. Spudich, K.-H. Jung, Microbial rhodopsins: phylogenetic and functional diversity, Handbook of Photosensory Receptors, Wiley-VCH Verlag GmbH & Co. KGaA 2005, pp. 1–23.
- [2] L.S. Brown, Eubacterial rhodopsins—unique photosensors and diverse ion pumps, Biochim. Biophys. Acta Bioenerg. 1837 (2014) 553–561.
- [3] O.P. Ernst, D.T. Lodowski, M. Elstner, P. Hegemann, L.S. Brown, H. Kandori, Microbial and animal rhodopsins: structures, functions, and molecular mechanisms, Chem. Rev. 114 (2014) 126–163.
- [4] J.K. Lanyi, Bacteriorhodopsin, Annu. Rev. Physiol. 66 (2004) 665–688.
- [5] H. Luecke, B. Schobert, J.-P. Cartailler, H.-T. Richter, A. Rosengarth, R. Needleman, J.K. Lanyi, Coupling photoisomerization of retinal to directional transport in bacteriorhodopsin, J. Mol. Biol. 300 (2000) 1237–1255.
- [6] O.A. Sineshchekov, K.-H. Jung, J.L. Spudich, Two rhodopsins mediate phototaxis to low- and high-intensity light in *Chlamydomonas reinhardtii*, Proc. Natl. Acad. Sci. 99 (2002) 8689–8694.
- [7] G. Nagel, D. Ollig, M. Fuhrmann, S. Kateriya, A.M. Mustl, E. Bamberg, P. Hegemann, Channelrhodopsin-1: a light-gated proton channel in green algae, Science 296 (2002) 2395–2398.
- [8] R. Moukhametzianov, J.P. Klare, R. Efremov, C. Baeken, A. Goppner, J. Labahn, M. Engelhard, G. Buldt, V.I. Gordelyi, Development of the signal in sensory rhodopsin and its transfer to the cognate transducer, Nature 440 (2006) 115–119.
- [9] S.P. Balashov, Protonation reactions and their coupling in bacteriorhodopsin, Biochim. Biophys. Acta Bioenerg. 1460 (2000) 75–94.
- [10] S. Wolf, E. Freier, M. Potschies, E. Hofmann, K. Gerwert, Directional proton transfer in membrane proteins achieved through protonated protein-bound water molecules: a proton diode, Angew. Chem. Int. Ed. 49 (2010) 6889–6893.
- [11] X. Ge, M.R. Gunner, Unraveling the mechanism of proton translocation in the extracellular half-channel of bacteriorhodopsin, Proteins 84 (2016) 639–654.
- [12] S. Subramaniam, T. Marti, H.G. Khorana, Protonation state of asp (Glu)-85 regulates the purple-to-blue transition in bacteriorhodopsin mutants Arg-82 \rightarrow Ala and Asp-85 \rightarrow Glu: the blue form is inactive in proton translocation, Proc. Natl. Acad. Sci. 87 (1990) 1013–1017.
- [13] H. Otto, T. Marti, M. Holtz, T. Mogi, M. Lindau, H.G. Khorana, M.P. Heyn, Aspartic acid-96 is the internal proton donor in the reprotonation of the Schiff base of bacteriorhodopsin, Proc. Natl. Acad. Sci. 86 (1989) 9228–9232.
- [14] L. Brown, Proton transport mechanism of bacteriorhodopsin as revealed by site-specific mutagenesis and protein sequence variability, Biochem. Mosc. 66 (2001) 1249–1255.
- [15] J.K. Lanyi, Proton transfers in the bacteriorhodopsin photocycle, Biochim. Biophys. Acta Bioenerg. 1757 (2006) 1012–1018.
- [16] O. Bèjà, L. Aravind, E.V. Koonin, M.T. Suzuki, A. Hadd, L.P. Nguyen, S.B. Jovanovich, C.M. Gates, R.A. Feldman, J.L. Spudich, E.N. Spudich, E.F. DeLong, Bacterial rhodopsin: evidence for a new type of phototrophy in the sea, Science 289 (2000) 1902–1906.
- [17] S.P. Balashov, E.S. Imasheva, V.A. Boichenko, J. Antón, J.M. Wang, J.K. Lanyi, Xanthorhodopsin: a proton pump with a light-harvesting carotenoid antenna, Science 309 (2005) 2061–2064.
- [18] V.B. Bergo, O.A. Sineshchekov, J.M. Kralj, R. Partha, E.N. Spudich, K.J. Rothschild, J.L. Spudich, His-75 in proteorhodopsin, a novel component in light-driven proton translocation by primary pumps, J. Biol. Chem. 284 (2009) 2836–2843.
- [19] H. Luecke, B. Schobert, J. Stagno, E.S. Imasheva, J.M. Wang, S.P. Balashov, J.K. Lanyi, Crystallographic structure of xanthorhodopsin, the light-driven proton pump with a dual chromophore, Proc. Natl. Acad. Sci. 105 (2008) 16561–16565.
- [20] C. Bamann, E. Bamberg, J. Wachtveitl, C. Glaubitz, Proteorhodopsin, Biochim. Biophys. Acta Bioenerg. 1837 (2014) 614–625.
- [21] A.K. Dioumaev, L.S. Brown, J. Shih, E.N. Spudich, J.L. Spudich, J.K. Lanyi, Proton transfers in the photochemical reaction cycle of proteorhodopsin, Biochemistry 41 (2002) 5348–5358.
- [22] H.G. Khorana, Two light-transducing membrane proteins: bacteriorhodopsin and the mammalian rhodopsin, Proc. Natl. Acad. Sci. 90 (1993) 1166–1171.
- [23] A. Miller, D. Oesterhelt, Kinetic optimization of bacteriorhodopsin by aspartic acid 96 as an internal proton donor, Biochim. Biophys. Acta Bioenerg. 1020 (1990) 57–64.
- [24] L.E. Petrovskaya, E.P. Lukashev, V.V. Chupin, S.V. Sychev, E.N. Lyukmanova, E.A. Kryukova, R.H. Ziganshin, E.V. Spirina, E.M. Rivkina, R.A. Khatypov, L.G. Erokhina, D.A. Gilichinsky, V.A. Shuvalov, M.P. Kirpichnikov, Predicted bacteriorhodopsin from *Exiguobacterium sibiricum* is a functional proton pump, FEBS Lett. 584 (2010) 4193–4196.
- [25] L. Petrovskaya, S. Balashov, E. Lukashev, E. Imasheva, I.Y. Gushchin, A. Dioumaev, A. Rubin, D. Dolgikh, V. Gordelyi, J. Lanyi, ESR—a retinal protein with unusual properties from *Exiguobacterium sibiricum*, Biochem. Mosc. 80 (2015) 688–700.
- [26] V. Iverson, R.M. Morris, C.D. Frazier, C.T. Berthiaume, R.L. Morales, E.V. Armbrust, Untangling genomes from metagenomes: revealing an uncultured class of marine *Euryarchaeota*, Science 335 (2012) 587–590.
- [27] V.H. Albarracín, I. Kraiselburd, C. Bamann, P.G. Wood, E. Bamberg, M.E. Farias, W. Gärtner, Functional green-tuned proteorhodopsin from modern stromatolites, PLoS One 11 (2016) e0154962.
- [28] D.F. Rodrigues, J. Goris, T. Vishnivetskaya, D. Gilichinsky, M.F. Thomashow, J.M. Tiedje, Characterization of *Exiguobacterium* isolates from the Siberian permafrost. Description of *Exiguobacterium sibiricum* sp. nov., Extremophiles 10 (2006) 285–294.
- [29] R.H. Lozier, R.A. Bogomolni, W. Stoekenius, Bacteriorhodopsin: a light-driven proton pump in *Halobacterium halobium*, Biophys. J. 15 (1975) 955–963.
- [30] S.P. Balashov, L.E. Petrovskaya, E.P. Lukashev, E.S. Imasheva, A.K. Dioumaev, J.M. Wang, S.V. Sychev, D.A. Dolgikh, A.B. Rubin, M.P. Kirpichnikov, J.K. Lanyi, Aspartate-histidine interaction in the retinal schiff base counterion of the light-driven proton pump of *Exiguobacterium sibiricum*, Biochemistry 51 (2012) 5748–5762.
- [31] A.K. Dioumaev, L.E. Petrovskaya, J.M. Wang, S.P. Balashov, D.A. Dolgikh, M.P. Kirpichnikov, J.K. Lanyi, Photocycle of *Exiguobacterium sibiricum* rhodopsin characterized by low-temperature trapping in the IR and time-resolved studies in the visible, J. Phys. Chem. B 117 (2013) 7235–7253.
- [32] S.P. Balashov, L.E. Petrovskaya, E.S. Imasheva, E.P. Lukashev, A.K. Dioumaev, J.M. Wang, S.V. Sychev, D.A. Dolgikh, A.B. Rubin, M.P. Kirpichnikov, J.K. Lanyi, Breaking the carboxyl rule: lysine 96 facilitates reprotonation of the Schiff base in the photocycle of a retinal protein from *Exiguobacterium sibiricum*, J. Biol. Chem. 288 (2013) 21254–21265.

- [33] I. Gushchin, P. Chervakov, P. Kuzmichev, A.N. Popov, E. Round, V. Borshchevskiy, A. Ishchenko, L. Petrovskaya, V. Chupin, D.A. Dolgikh, A.S. Arseniev, M. Kirpichnikov, V. Gordeljiy, Structural insights into the proton pumping by unusual proteorhodopsin from nonmarine bacteria, *Proc. Natl. Acad. Sci.* 110 (2013) 12631–12636.
- [34] M.R. Gunner, J. Mao, Y. Song, J. Kim, Factors influencing the energetics of electron and proton transfers in proteins. What can be learned from calculations, *Biochim. Biophys. Acta Bioenerg.* 1757 (2006) 942–968.
- [35] A.K. Dioumaev, J.M. Wang, Z. Bálint, G. Váró, J.K. Lanyi, Proton transport by proteorhodopsin requires that the retinal Schiff base counterion asp-97 be anionic, *Biochemistry* 42 (2003) 6582–6587.
- [36] S.P. Balashov, E.S. Imasheva, T.G. Ebrey, N. Chen, D.R. Menick, R.K. Crouch, Glutamate-194 to cysteine mutation inhibits fast light-induced proton release in bacteriorhodopsin, *Biochemistry* 36 (1997) 8671–8676.
- [37] P. Läuger, *Electrogenic Ion Pumps*, Sinauer Associates, 1991.
- [38] L.A. Drachev, A.A. Jasaitis, A.D. Kaulen, A.A. Kondrashin, E.A. Liberman, I.B. Nemecek, S.A. Ostroumov, A.Y. Semenov, V.P. Skulachev, Direct measurement of electric current generation by cytochrome oxidase, H^+ -ATPase and bacteriorhodopsin, *Nature* 249 (1974) 321–324.
- [39] L.A. Drachev, A.D. Kaulen, L.V. Khitrina, V.P. Skulachev, Fast stages of photoelectric processes in biological membranes. I. Bacteriorhodopsin, *Eur. J. Biochem./FEBS Lett.* 117 (1981) 461–470.
- [40] I. Kalaïdzidis, A. Kaulen, A. Radionov, L. Khitrina, Photoelectrochemical cycle of bacteriorhodopsin, *Biochem. Mosc.* 66 (2001) 1220–1233.
- [41] A. Dér, L. Keszhelyi, Charge motion during the photocycle of bacteriorhodopsin, *Biochem. Mosc.* 66 (2001) 1234–1248.
- [42] O.P. Kaminskaya, L.A. Drachev, A.A. Konstantinov, A.Y. Semenov, V.P. Skulachev, Electrogenic reduction of the secondary quinone acceptor in chromatophores of *Rhodospirillum rubrum*: rapid kinetics measurements, *FEBS Lett.* 202 (1986) 224–228.
- [43] S.M. Dracheva, L.A. Drachev, A.A. Konstantinov, A.Y. Semenov, V.P. Skulachev, A.M. Arutjunjan, V.A. Shuvalov, S.M. Zaberezhnaya, Electrogenic steps in the redox reactions catalyzed by photosynthetic reaction-centre complex from *Rhodospseudomonas viridis*, *Eur. J. Biochem.* 171 (1988) 253–264.
- [44] L. Drachev, O. Kaminskaya, A. Konstantinov, M. Mamedov, V. Samuilov, A.Y. Semenov, V. Skulachev, Effects of electron donors and acceptors on the kinetics of the photoelectric responses in *Rhodospirillum rubrum* and *Rhodospseudomonas sphaeroides* chromatophores, *Biochim. Biophys. Acta Bioenerg.* 850 (1986) 1–9.
- [45] L. Drachev, B. Kaurav, M. Mamedov, A.Y. Mulikdjanian, A.Y. Semenov, V. Shinkarev, V. Skulachev, M. Verkhovskiy, Flash-induced electrogenic events in the photosynthetic reaction center and bc 1 complexes of *Rhodobacter sphaeroides* chromatophores, *Biochim. Biophys. Acta Bioenerg.* 973 (1989) 189–197.
- [46] M.D. Mamedov, O.E. Beshta, V.D. Samuilov, A.Y. Semenov, Electrogenicity at the secondary quinone acceptor site of cyanobacterial photosystem II, *FEBS Lett.* 350 (1994) 96–98.
- [47] M. Mamedov, R. Gadzhieva, K. Gourvovskaya, L. Drachev, A.Y. Semenov, Electrogenicity at the donor/acceptor sides of cyanobacterial photosystem I, *J. Bioenerg. Biomembr.* 28 (1996) 517–522.
- [48] D. Zaslavsky, I. Smirnova, S. Siletsky, A. Kaulen, F. Millett, A. Konstantinov, Rapid kinetics of membrane potential generation by cytochrome *c* oxidase with the photoactive Ru (II)-tris-bipyridyl derivative of cytochrome *c* as electron donor, *FEBS Lett.* 359 (1995) 27–30.
- [49] S. Siletsky, A.D. Kaulen, A.A. Konstantinov, Resolution of electrogenic steps coupled to conversion of cytochrome *c* oxidase from the peroxy to the ferryl-oxo state, *Biochemistry* 38 (1999) 4853–4861.
- [50] A. Jasaitis, M.I. Verkhovskiy, J.E. Morgan, M.L. Verkhovskaya, M. Wikström, Assignment and charge translocation stoichiometries of the major electrogenic phases in the reaction of cytochrome *c* oxidase with dioxygen, *Biochemistry* 38 (1999) 2697–2706.
- [51] S.A. Siletsky, J. Zhu, R.B. Gennis, A.A. Konstantinov, Partial steps of charge translocation in the nonpumping N139L mutant of *Rhodobacter sphaeroides* cytochrome *c* oxidase with a blocked D-channel, *Biochemistry* 49 (2010) 3060–3073.
- [52] S.A. Siletsky, A.A. Konstantinov, Cytochrome *c* oxidase: charge translocation coupled to single-electron partial steps of the catalytic cycle, *Biochim. Biophys. Acta Bioenerg.* 1817 (2012) 476–488.
- [53] A.V. Bogachev, Y.V. Bertsova, M.L. Verkhovskaya, M.D. Mamedov, V.P. Skulachev, Real-time kinetics of electrogenic Na^+ transport by rhodopsin from the marine flavobacterium *Dokdonia* sp. PRO95, *Sci. Rep.* 6 (2016) 21397.
- [54] L. Drachev, A. Kaulen, V. Skulachev, Correlation of photochemical cycle, H^+ release and uptake, and electric events in bacteriorhodopsin, *FEBS Lett.* 178 (1984) 331–335.
- [55] A.D. Kaulen, Electrogenic processes and protein conformational changes accompanying the bacteriorhodopsin photocycle, *Biochim. Biophys. Acta Bioenerg.* 1460 (2000) 204–219.
- [56] T. Friedrich, S. Geibel, R. Kalmbach, I. Chizhov, K. Ataka, J. Heberle, M. Engelhard, E. Bamberg, Proteorhodopsin is a light-driven proton pump with variable vectoriality, *J. Mol. Biol.* 321 (2002) 821–838.
- [57] O.A. Sineshchekov, J.L. Spudich, Light-induced intramolecular charge movements in microbial rhodopsins in intact *E. coli* cells, *Photochem. Photobiol. Sci.* 3 (2004) 548–554.
- [58] A. Vogt, J. Wietek, P. Hegemann, Gloeobacter rhodopsin, limitation of proton pumping at high electrochemical load, *Biophys. J.* 105 (2013) 2055–2063.
- [59] J.-L. Rigaud, B. Pitard, D. Levy, Reconstitution of membrane proteins into liposomes: application to energy-transducing membrane proteins, *Biochim. Biophys. Acta Bioenerg.* 1231 (1995) 223–246.
- [60] R. Tunuguntla, M. Bangar, K. Kim, P. Stroeve, C.M. Ajo-Franklin, A. Noy, Lipid bilayer composition can influence the orientation of proteorhodopsin in artificial membranes, *Biophys. J.* 105 (2013) 1388–1396.
- [61] D. Zaslavsky, A.D. Kaulen, I.A. Smirnova, T. Vygodina, A.A. Konstantinov, Flash-induced membrane potential generation by cytochrome *c* oxidase, *FEBS Lett.* 336 (1993) 389–393.
- [62] A.A. Konstantinov, S. Siletsky, D. Mitchell, A. Kaulen, R.B. Gennis, The roles of the two proton input channels in cytochrome *c* oxidase from *Rhodobacter sphaeroides* probed by the effects of site-directed mutations on time-resolved electrogenic intraprotein proton transfer, *Proc. Natl. Acad. Sci.* 94 (1997) 9085–9090.
- [63] S.A. Siletsky, A.S. Pawate, K. Weiss, R.B. Gennis, A.A. Konstantinov, Transmembrane charge separation during the ferryl-oxo \rightarrow oxidized transition in a nonpumping mutant of cytochrome *c* oxidase, *J. Biol. Chem.* 279 (2004) 52558–52565.
- [64] D. Medvedev, A. Kotelnikov, A. Stuchebrukhov, Analysis of the kinetics of the membrane potential generated by cytochrome *c* oxidase upon single electron injection, *Biochim. Biophys. Acta Bioenerg.* 1710 (2005) 47–56.
- [65] S.A. Siletsky, D. Han, S. Brand, J.E. Morgan, M. Fabian, L. Geren, F. Millett, B. Durham, A.A. Konstantinov, R.B. Gennis, Single-electron photoreduction of the PM intermediate of cytochrome *c* oxidase, *Biochim. Biophys. Acta Bioenerg.* 1757 (2006) 1122–1132.
- [66] S.A. Siletsky, Steps of the coupled charge translocation in the catalytic cycle of cytochrome *c* oxidase, *Front. Biosci. (Landmark Ed.)* 18 (2012) 36–57.
- [67] S.A. Siletsky, I. Belevich, A. Jasaitis, A.A. Konstantinov, M. Wikström, T. Soulimane, M.I. Verkhovskiy, Time-resolved single-turnover of ba 3 oxidase from *Thermus thermophilus*, *Biochim. Biophys. Acta Bioenerg.* 1767 (2007) 1383–1392.
- [68] S.A. Siletsky, I. Belevich, T. Soulimane, M.I. Verkhovskiy, M. Wikström, The fifth electron in the fully reduced caa 3 from *Thermus thermophilus* is competent in proton pumping, *Biochim. Biophys. Acta Bioenerg.* 1827 (2013) 1–9.
- [69] I. Belevich, E. Gorbikova, N.P. Belevich, V. Rauhamaäki, M. Wikström, M.I. Verkhovskiy, Initiation of the proton pump of cytochrome *c* oxidase, *Proc. Natl. Acad. Sci.* 107 (2010) 18469–18474.
- [70] Y.L. Kalaïdzidis, A. Gavrilov, P. Zaitsev, A. Kalaïdzidis, E. Korolev, PLUK—an environment for software development, *Program. Comput. Softw.* 23 (1997) 206–211.
- [71] J. Tamogami, K. Sato, S. Kurokawa, T. Yamada, T. Nara, M. Demura, S. Miyauchi, T. Kikukawa, E. Muneyuki, N. Kamo, Formation of M-like intermediates in proteorhodopsin in alkali solutions (pH \geq 8.5) where the proton release occurs first in contrast to the sequence at lower pH, *Biochemistry* 55 (2016) 1036–1048.
- [72] C. Zscherp, R. Schlesinger, J. Tittor, D. Oesterheld, J. Heberle, In situ determination of transient pKa changes of internal amino acids of bacteriorhodopsin by using time-resolved attenuated total reflection Fourier-transform infrared spectroscopy, *Proc. Natl. Acad. Sci.* 96 (1999) 5498–5503.
- [73] M. Kono, S. Misra, T.G. Ebrey, pH dependence of light-induced proton release by bacteriorhodopsin, *FEBS Lett.* 331 (1993) 31–34.
- [74] S. Dickopf, M.P. Heyn, Evidence for the first phase of the reprotonation switch of bacteriorhodopsin from time-resolved photovoltage and flash photolysis experiments on the photoreversal of the M-intermediate, *Biophys. J.* 73 (1997) 3171.
- [75] A.L. Drachev, L.A. Drachev, A.D. Kaulen, L.V. Khitrina, The action of lanthanum ions and formaldehyde on the proton-pumping function of bacteriorhodopsin, *Eur. J. Biochem.* 138 (1984) 349–356.
- [76] S.P. Balashov, M. Lu, E.S. Imasheva, R. Govindjee, T.G. Ebrey, B. Othersen III, R.K. Crouch, D.R. Menick, The proton release group in bacteriorhodopsin controls the rate of the final step of its photocycle at low pH, *Biochemistry* 38 (1999) 2026–2039.
- [77] L.S. Brown, J.K. Lanyi, Determination of the transiently lowered pK_a of the retinal Schiff base during the photocycle of bacteriorhodopsin, *Proc. Natl. Acad. Sci.* 93 (1996) 1731–1734.
- [78] L. Khitrina, A. Ksenofontov, Bacteriorhodopsin. Correspondence of the photocycle and electrogenesis with sites of the molecule, *Biochem. Mosc.* 69 (2004) 1407–1409.